New Phytologist

Xylem traits mediate a trade-off between resistance to freeze–thaw-induced embolism and photosynthetic capacity in overwintering evergreens

Brendan Choat[1], Danielle E. Medek[1], Stephanie A. Stuart[1], Jessica Pasquet-Kok[2], John J. G. Egerton[1], Hooman Salari[1], Lawren Sack[2] and Marilyn C. Ball[1]

[1]Plant Science Division, Research School of Biology, The Australian National University, Canberra, ACT 0200, Australia; [2]Department of Ecology and Evolutionary Biology, University of California, Los Angeles, 621 Charles E. Young Drive South, Los Angeles, CA 90095-1606, USA

Author for correspondence:
Marilyn C. Ball
Tel: +61 2 6125 5057
Email: marilyn.ball@anu.edu.au

Received: *9 March 2011*
Accepted: *7 April 2011*

New Phytologist (2011) **191**: 996–1005
doi: 10.1111/j.1469-8137.2011.03772.x

Key words: cavitation, embolism, evergreen, freezing, hydraulic conductivity, photosynthesis, xylem.

Summary

• Hydraulic traits were studied in temperate, woody evergreens in a high-elevation heath community to test for trade-offs between the delivery of water to canopies at rates sufficient to sustain photosynthesis and protection against disruption to vascular transport caused by freeze–thaw-induced embolism.

• Freeze–thaw-induced loss in hydraulic conductivity was studied in relation to xylem anatomy, leaf- and sapwood-specific hydraulic conductivity and gas exchange characteristics of leaves.

• We found evidence that a trade-off between xylem transport capacity and safety from freeze–thaw-induced embolism affects photosynthetic activity in overwintering evergreens. The mean hydraulically weighted xylem vessel diameter and sapwood-specific conductivity correlated with susceptibility to freeze–thaw-induced embolism. There was also a strong correlation of hydraulic supply and demand across species; interspecific differences in stomatal conductance and CO_2 assimilation rates were correlated linearly with sapwood- and leaf-specific hydraulic conductivity.

• Xylem vessel anatomy mediated an apparent trade-off between resistance to freeze–thaw-induced embolism and hydraulic and photosynthetic capacity during the winter. These results point to a new role for xylem functional traits in determining the degree to which species can maintain photosynthetic carbon gain despite freezing events and cold winter temperatures.

Introduction

Low temperatures are important determinants of species' distributions, with freezing presenting major challenges to evergreen species in frost-prone climates (Sakai & Larcher, 1987). Woody plants that tolerate freezing undergo seasonal changes in acclimation which enable living cells to tolerate the dehydration that accompanies extracellular ice formation (Xin & Browse, 2000). In addition, water transport to leaves is threatened when xylem conduits become embolized following freeze–thaw events (Hacke & Sperry, 2001). Such a loss of water transport can reduce the capacity of a plant to take advantage of warm, sunny conditions, particularly when growth recommences in spring. Hence, among woody evergreens, interspecific differences in vulnerability to freeze–thaw-induced embolism could influence growth, competitive outcomes and distribution along gradients in minimum temperature. Although freeze–thaw-induced embolism has been studied in a variety of species (Sperry *et al.*, 1994; Langan *et al.*, 1997; Cavender-Bares & Holbrook, 2001; Feild & Brodribb, 2001; Ball *et al.*, 2006), its influence on carbon balance is not well understood.

The mechanism of freeze–thaw-induced embolism differs from that of drought-induced tension (Hacke & Sperry, 2001). Ice is crystalline and the solubilities of gases in ice are much lower than in liquid water. Consequently, when water freezes, gases dissolved in water can be forced out of solution, forming bubbles surrounded by ice. When frozen xylem sap thaws, bubbles formed during freezing can either

dissolve (in water released by melting ice) or expand until the xylem conduit is filled with gas, a process known as cavitation. According to the Young–Laplace equation, whether a bubble dissolves or nucleates a cavitation depends on its internal pressure (P_B), which is a function of its radius (r), the surface tension of xylem sap (γ) and the pressure of xylem sap (P_x), where $P_B = (2\gamma/r) + P_x$. Small bubbles or those subject to large positive external pressure tend to collapse or to dissolve, and so the probability that a bubble will nucleate a cavitation increases with an increase in the radius of curvature of the bubble and the tension in the xylem stream. These two components are highly variable. Values of r are thought to depend on the size of xylem conduits; larger conduits contain more water and hence more air is forced out of solution during freezing, thereby increasing the probability that a bubble with a critical radius for nucleation will form on thawing (Sperry & Sullivan, 1992). Indeed, many studies have reported that narrow conduits have an advantage in resisting freeze–thaw-induced embolism (Sperry & Sullivan, 1992; Logullo & Salleo, 1993; Davis *et al.*, 1999; Pittermann & Sperry, 2003; Stuart *et al.*, 2007). Such an advantage for narrow conduits contrasts with anatomical adaptations to maintaining xylem function during drought, which relate more to the structure of intervessel pits (Choat *et al.*, 2008). Although narrow conduits have lower probabilities of freeze–thaw-induced embolism (Davis *et al.*, 1999), they may impose a limit on the carbon and water economy of plants when conditions are favourable for photosynthesis and growth. A small reduction in conduit diameter considerably decreases vessel conductivity, because, as the Hagen–Poiseuille equation states, conductivity is proportional to vessel radius raised to the fourth power (Tyree & Zimmermann, 2002). Thus, narrow conduits that benefit resistance to freeze–thaw-induced embolism involve a trade-off in maximum hydraulic conductivity (Wang *et al.*, 1992; Sperry *et al.*, 1994; Feild & Brodribb, 2001).

Such a trade-off would mean that narrow conduits may also limit growth (Castro-Diez *et al.*, 1998). Although the role of stomata in regulating water loss and photosynthetic rates is well established (Givnish, 1986), the hydraulic architecture and hydraulic conductivity of stem xylem (K_s) may also constrain the productivity of trees (Zhang & Cao, 2009). Indeed, there is increasing evidence of functional coordination between the hydraulic capacity of stems to supply water to leaves and the gas exchange characteristics of leaves (Meinzer *et al.*, 1995; Franks & Farquhar, 1999; Hubbard *et al.*, 2001; Sack & Holbrook, 2006). These relationships are complicated by allocation patterns that affect leaf-specific conductivity K_L [K_s multiplied by the sapwood : leaf area ratio, i.e. the Huber value (HV)], the most direct metric for the influence of stem conductivity on leaf gas exchange (Brodribb *et al.*, 2003; Santiago *et al.*, 2004). For example, even a stem with low K_s can support a high stomatal conductance and favourable rates of CO_2 assimilation without causing tension-induced cavitation if K_L is sufficiently high (i.e. if the stem supports less leaf area for a given K_s). Thus, if hydraulic traits associated with the minimization of freeze–thaw-induced embolism constrain the rate of delivery of water to leaves, we predict that morphological adaptations that alter the scaling between photosynthetic and nonphotosynthetic tissues will have significant impacts on productivity.

Although the coordination of hydraulic and photosynthetic traits has been demonstrated in a number of studies, these have typically focused on optimal conditions during the primary growing season (Brodribb & Feild, 2000; Santiago *et al.*, 2004; Chen *et al.*, 2009), and there have been no such studies to our knowledge for woody plants facing winter. In the boreal zone, evergreen plants have low and often negligible photosynthetic rates during the winter (Mooney & Ehleringer, 1997). However, in the temperate zone, winter photosynthetic activity may contribute significantly to annual growth in broadleaf evergreens (Miyazawa & Kikuzawa, 2005). In Australia, winter photosynthesis supports root growth (Blennow *et al.*, 1998; Egerton *et al.*, 2000) and contributes substantially to the rapid growth of eucalypts during early spring when soil resources are relatively abundant (Ball *et al.*, 1997). Hence, the ability to resist freeze–thaw-induced embolism may be a strong benefit for overwintering evergreens, although few data are available.

We examined the interrelationships between resistance to freeze–thaw-induced embolism, hydraulic capacity and leaf gas exchange in a high-elevation heath community dominated by evergreen angiosperms regularly exposed to winter freezing. The wide range of growth forms and diverse xylem structure present in the heath flora provided an ideal opportunity to study the functional diversity of adaptation in hydraulic traits to low-temperature stress. Measurements of xylem vessel diameter and hydraulic conductivity were made in conjunction with experimental manipulations to determine the loss of hydraulic capacity associated with a severe freeze–thaw event, and were related to field measurements of stomatal conductance and CO_2 assimilation rates. We tested three key hypotheses of hydraulic limitation in this system: that stem hydraulic conductivity is negatively related to resistance to freeze–thaw-induced embolism; that stem hydraulic conductivity correlates across species with leaf gas exchange; and that this variation in xylem vessel diameter underlies both relationships.

Materials and Methods

Study site

Field measurements were made in July (mid-winter) 2009 in Kanangra Boyd National Park (33°59′9″S,

Table 1 Species and families selected from heath vegetation with average species' height at site

Species	Family	Growth form	Height (m)
Acacia obtusifolia (Ao)	Fabaceae	Tree	3
Allocasuarina littoralis (Al)	Casuarinaceae	Tree	6
Baeckia brevifolia (Bb)	Myrtaceae	Shrub	2
Banksia ericifolia (Be)	Proteaceae	Tree	2
Banksia spinulosa (Bs)	Proteaceae	Tree	2
Eucalyptus burgessiana (Eb)	Myrtaceae	Tree	10
Eucalyptus sieberi (Es)	Myrtaceae	Tree	15
Hakea dactyloides (Hd)	Proteaceae	Tree	3
Isopogon anemonifolius (Ia)	Proteaceae	Shrub	1
Leptospermum polygalifolium (Lp)	Myrtaceae	Tree	2
Petrophile pulchella (Pp)	Proteaceae	Shrub	2

150°6′37″E), within the Greater Blue Mountains World Heritage Area in south-eastern Australia. The site was located on an exposed plateau at 1070 m above sea level adjacent to the Kanangra Walls. No weather data are available for this remote site. The closest weather station is located *c.* 20 km from the site at Oberon (elevation 1190 m above sea level) in very different topography, and so gives an indication of regional conditions. Oberon receives a mean annual rainfall of 725 mm yr^{-1} distributed evenly throughout the year. The mean maximum and minimum air temperatures are 16.2 and 6.2°C, respectively. In the winter months (June, July, August), average minimum temperatures range between 0.5 and 1.6°C and the lowest recorded minimum air temperature is −7.5°C (Australian Bureau of Meteorology, 2011). The site therefore provides a combination of chilling and freezing temperatures and high levels of hydration during winter.

Eleven shrub and tree species were selected from the heath vegetation on Boyd Plateau, which is dominated by species from the Proteaceae and Myrtaceae, as well as *Acacia* and *Allocasuarina* (Table 1). Three individuals of each species were selected for measurements of anatomy, hydraulic traits and leaf gas exchange.

Xylem anatomy

Branch samples were collected for each species before dawn and returned to the field laboratory. For each of the 11 species, we measured the maximum vessel length using the air injection technique (Zimmermann and Jeje 1981). Branch samples of 5–10 mm in diameter were stored in 50% ethanol for anatomical analysis. Transverse sections were then taken on a sliding microtome and observed under a compound microscope (Nikon, Tokyo, Japan). Images were collected using a digital camera (Canon Powershot S5; Canon, Tokyo, Japan) and analysed using imageJ software (US National Institutes of Health, Bethesda, MD, USA). A region of sapwood from pith to cambium was examined, and the xylem diameter was estimated by measuring the areas of the vessel lumens in transverse section and calculating the diameter of a circle with the same area. Conduits with diameters < 5 μm were excluded from the analysis. The hydraulically weighted vessel diameter (D_h) was calculated as $D_h = (\Sigma D^4/N)^{1/4}$, where N is the number of vessels in cross-section (Tyree & Zimmermann, 2002).

Hydraulic conductivity and freeze–thaw-induced embolism

Branch sections longer than the longest vessel were collected before dawn, placed into plastic bags with moist paper towels and returned to the field laboratory, a 30 min drive away. For each replicate individual, two branches were collected, one for the freeze–thaw treatment and one as an untreated control. In the laboratory, branches were separated into two groups. Treatment branches were placed into an insulated freezing chamber (Stuart *et al.*, 2007) and control braches were left in plastic bags for the duration of the treatment. The temperature of the freezing chamber was controlled by a programmable water bath (Julabo, Seelbach, Germany). The air temperature of the chamber and the temperature of stems and leaves were monitored throughout the experiment by copper-constantan thermocouples (64 μm in diameter) referenced against a platinum resistance thermometer and connected to a DT800 Datataker (Datataker, Scoresby, Australia). The chamber was cooled from 2°C at a rate of 2°C per hour, with stems reaching average nadir temperatures of −7.5°C at the conclusion of the freezing cycle (Table 2). Freezing exotherms were recorded first in the leaves in almost all cases at an average temperature of −4.8°C. Samples were held at the nadir temperature for 30 min, and then removed from the freezing chamber and allowed to thaw to room temperature over 30 min. Samples were placed back into humidified plastic

Table 2 Leaf nucleation temperature and nadir stem temperature for branches in freezing chamber (averages ± SE)

Species	Leaf nucleation temperature (°C)		Nadir stem temperature (°C)
Allocasuarina littoralis	−5.14	±0.51	−8.32
Acacia obtusifolia	−7.04	±0.64	−7.65
Baeckia brevifolia	−5.54		−7.00
Banksia ericifolia	−4.29	±0.31	−6.62
Banksia spinulosa	−5.45	±0.32	−8.24
Eucalyptus burgessiana	−3.33	±0.74	−7.81
Eucalyptus sieberi	−3.46	±0.43	−7.64
Hakea dactyloides	−4.79	±0.33	−7.46
Isopogon anemonifolius	−4.46	±0.39	−7.79
Leptospermum polygalifolium	−6.10	±1.10	−7.43
Petrophile pulchella	−3.72	±0.22	−7.08

bags whilst thawing. Because freeze–thaw-induced embolism can depend on the tension in the xylem during freezing, we characterized bagged leaf (stem) water potentials before freezing with a pressure chamber (Plant Moisture Stress, Albany, OR, USA).

Hydraulic conductivity was measured on branch sections, 5 cm in length and 5–10 mm in diameter, cut from treatment and control branches under water and trimmed with a fresh razor blade. Segments were connected to water-filled tubing running to a reservoir raised above the stems to deliver 5 kPa of hydraulic pressure. The perfusate used was 10 mM KCl, filtered to 0.2 μm with Millipore syringe filters (Millex GS Filter; Millipore Corrigtwohill Co, Cork, Ireland). The rate of water flow through the stems was measured by tracking the movement of the meniscus in a calibrated pipette connected by tubing to the distal end of the stem. The position of the meniscus was recorded every 30 s by a digital camera (Canon Powershot G10) connected to a laptop computer (using Canon Utilities RemoteCapture DC version 3.1.0.5; Canon). The flow rate was measured for 10–20 min, with the final flow rate value averaged over a 3 min period once the flow had stabilized. After an initial flow rate measurement, the samples were flushed at a pressure of 125 kPa for 20 min to remove emboli. The flow rate was then measured again to determine the maximum conductivity and the loss of conductivity caused by embolism. The hydraulic conductivity (K_h) was calculated as $K_h = FL/\Delta P$, where F is the flow rate, L is the segment length and ΔP is the pressure difference across the sample. The leaf area distal to the segment (A_L) and the conductive sapwood area (A_s) were also measured to calculate the sapwood-specific hydraulic conductivity (K_s) and leaf-specific hydraulic conductivity (K_L) as $K_s = K_h/A_s$ and $K_L = K_h/A_L$, respectively. The percentage loss of hydraulic conductivity (PLC) was calculated as $PLC = (K_{max} - K_{initial})/K_{max} \times 100$, where $K_{initial}$ and K_{max} are the initial and maximum hydraulic conductivities, respectively. The PLC caused by a freeze–thaw cycle was calculated as the PLC of treated branches minus the PLC of control branches. For each of the 11 species, a treatment branch and a control branch from each of three individuals were measured to determine the hydraulic parameters.

The segment length of 5 cm was chosen to allow for easy flushing of the segments and standardization across a broad range of branch morphology. It is recognized that open vessels occur in these short segments and that this will lead to higher values of K_s and K_L than in longer segments with no open vessels, because endwall resistance has been removed. Therefore, caution must be used when comparing these measurements directly with those made on longer segments with no open vessels. However, because lumen and pit resistances are coordinated across angiosperm species (Sperry *et al.*, 2005), it is expected that conductivity values obtained from short segments will hold their species' ranks for comparison with leaf gas exchange parameters.

Leaf gas exchange

Measurements of stomatal conductance and CO_2 assimilation rate were made during the morning from 09:00 to 11:00 h over a 3 wk period in July 2009 with an Li-Cor portable gas exchange system (Li-Cor 6400; Lincoln, NE, USA). Measurements were made on one block per week, with each block containing one individual of each of the 11 species. Measurements were made at ambient temperature and relative humidity with a photosynthetic photon flux density of 1200 μmol m^{-2} s^{-1} and a chamber flow rate of 400 μmol s^{-1}. There was no significant difference ($P = 0.48$) between species in leaf temperature, which ranged from average values of 9.6 ± 0.1°C for *Eucalyptus sieberi* to 11.4 ± 1.2°C for *Acacia obtusifolia*. The reference CO_2 concentration was maintained at 380 μmol mol^{-1} by the LI-6400 CO_2 injector using a high-pressure liquefied CO_2 cartridge.

Statistics

For initial and maximum values of K_s and K_L, and for xylem anatomical traits, differences among species were established using a general linear model with trait data averaged for each replicate tree ($n = 3$; SPSS Statistics 18; IBM Corporation, New York, NY, USA). To test the effect of the freeze–thaw treatments, we conducted a repeated-measures ANOVA, comparing the impact on each individual of each species, determining the effect of species, treatment and interaction (Minitab Pty. Ltd., Minitab Release 14; State College, PA, USA). Bivariate relationships were assessed using parametric correlation coefficients (r), and lines were fitted by linear regression or nonlinear curve fitting using the simplex procedure (Origin 8.1; OriginLab Corporation, Northampton, MA, USA).

Results

Xylem anatomy

Xylem anatomy varied significantly among the 11 species (Table 3). The mean hydraulically weighted vessel diameter (D_h) ranged from 14.1 μm in *Hakea dactyloides* to 33.3 μm in *E. sieberi*. The hydraulically weighted vessel diameter was negatively related to vessel density and positively related to maximum vessel length (L_{Vmax}) ($r = -0.79$, $P = 0.004$ and $r = 0.86$, $P < 0.001$, respectively) (Fig. 1).

Hydraulic conductivity and freeze–thaw-induced embolism

The sapwood-specific hydraulic conductivity (K_s) varied widely among the 11 species ($P < 0.001$; ANOVAs on initial and flushed stems), with two shrub species, *Isopogon*

anemonifolius and *Petrophile pulchella*, having the lowest values and the two *Eucalyptus* species having the highest values (Fig. 2a). For K_L, ranks were exchanged between the species because of variation in HV (Fig. 2b). HV increased with decreasing K_s following a power function (r^2 = 0.66, P < 0.0001), indicating that the species with less efficient sapwood tend to support their leaf area with greater cross-sectional area of stem (Fig. 3). Thus, HV tended to partially compensate for K_s differences and, as a result, K_L was less variable than K_s across species, and did not correlate significantly with K_s across species (Figs 2a,b, 3).

The loss of hydraulic conductivity induced by the experimental freeze–thaw treatment was significant across the species (repeated-measures ANOVA testing the percentage loss in conductivity between the control and treated shoots; species effect, P = 0.006; treatment, P = 0.001; species × treatment, P = 0.045). Freeze–thaw-induced loss of conductivity was negligible for *Baeckia brevifolia* and *Leptospermum polygalifolium* and varied from 4% for *I. anemonifolius* to 56% for *E. sieberi* (Fig. 4). Species with narrower vessels and lower conductivities were less vulnerable to freeze–thaw-induced embolism than species with wider vessels (Fig. 5); the magnitude of PLC caused by a freeze–thaw cycle was significantly related to D_h (r = 0.65, P = 0.03) and K_s (r = 0.71, P = 0.01). No relationship was observed across species between stem water potential before freezing and freeze–thaw-induced PLC; however, stem water potentials were relatively high (−0.15 to −0.98 MPa), and were above −0.5 MPa in all species except *B. brevifolia* (overall mean = −0.32 MPa; Table 3).

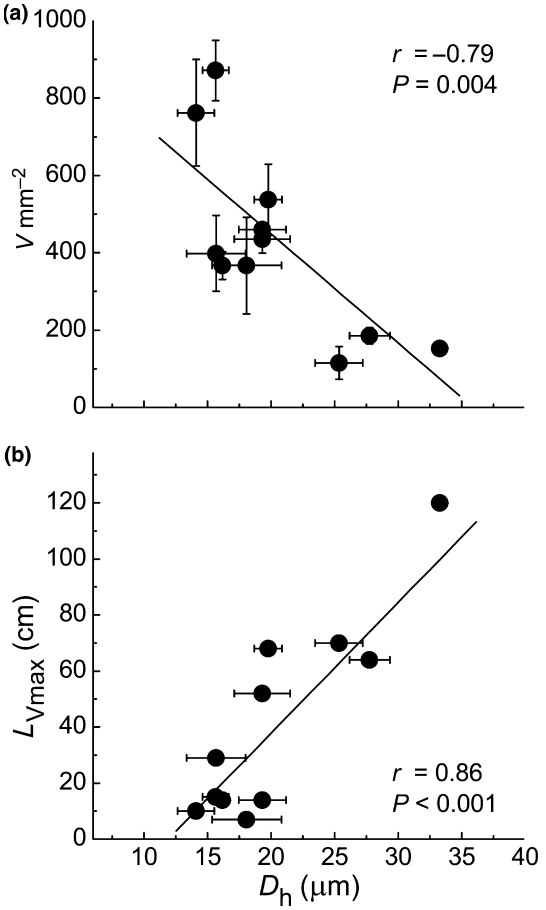

Fig. 1 (a) Hydraulically weighted vessel diameter (D_h) vs vessels per cross-sectional area of xylem (V mm^{-2}) and (b) D_h vs maximum vessel length (L_{Vmax}). Each point is the mean from three individuals (n = 3) with error bar showing standard error.

Relationships between leaf gas exchange and hydraulic traits

Stomatal conductance and CO_2 assimilation rates were significantly related to K_{Lmax} (r = 0.87, P < 0.001 and r = 0.73, P = 0.01, respectively) for untreated control branches (Fig. 6), demonstrating the association of leaf level gas exchange and the capacity of stem tissue to supply water to the leaves. Stomatal conductance and A were related to K_{smax} (r = 0.67, P = 0.02 and r = 0.71, P = 0.01, respec-

Table 3 Hydraulically weighted mean vessel diameter (D_h), vessel density (VD), maximum vessel length (L_{Vmax}) and stem water potential before freezing (Ψ_s) of 11 heath species

Species	D_h (μm)	VD	L_{Vmax} (cm)	Ψ_s (MPa)
Acacia obtusifolia	25.2 (2.0) bcd	115 (11) a	70	−0.46 (0.17)
Allocasuarina littoralis	19.8 (1.1) abc	537 (7) bcd	68	−0.24 (0.05)
Baeckia brevifolia	15.7 (2.3) a	398 (4) abc	29	−0.98 (0.42)
Banksia ericifolia	18.1 (2.7) ab	367 (17) abc	7	−0.15 (0.08)
Banksia spinulosa	19.3 (1.8) abc	460 (23) abc	14	−0.19 (0.09)
Eucalyptus burgessiana	27.8 (1.6) cd	185 (16) ab	64	−0.23 (0.09)
Eucalyptus sieberi	33.3 (0.4) d	152 (1) ab	120	−0.17 (0.09)
Hakea dactyloides	14.1 (1.4) a	762 (9) cd	10	−0.36 (0.13)
Isopogon anemonifolius	16.2 (0.5) a	367 (6) abc	14	−0.23 (0.03)
Leptospermum polygalifolium	19.3 (2.2) abc	436 (6) abc	52	−0.15 (0.08)
Petrophile pulchella	15.6 (1.0) a	872 (16) d	15	−0.33 (0.21)

Values are means from three individuals (n = 3) with SE in parentheses. Different lower case letters represent significant differences (P < 0.05) within each column.

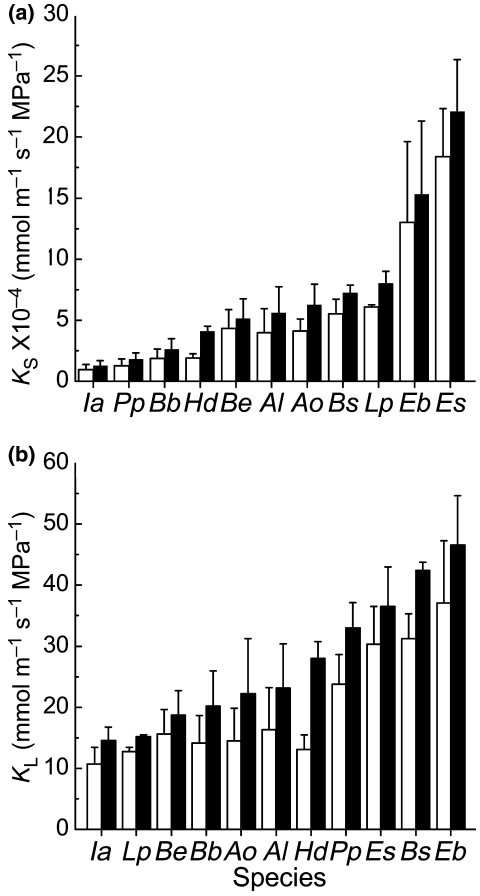

Fig. 2 Hydraulic conductivity of stems for 11 woody heath species. Initial (open bars) and maximum (closed bars) hydraulic conductivity is shown normalized to leaf area distal to the stem (K_s) (a) and xylem cross-sectional area (K_L) (b). Bars show mean values from three individuals (n = 3) with error bars showing standard error. Abbreviations of the species' names are given in Table 1.

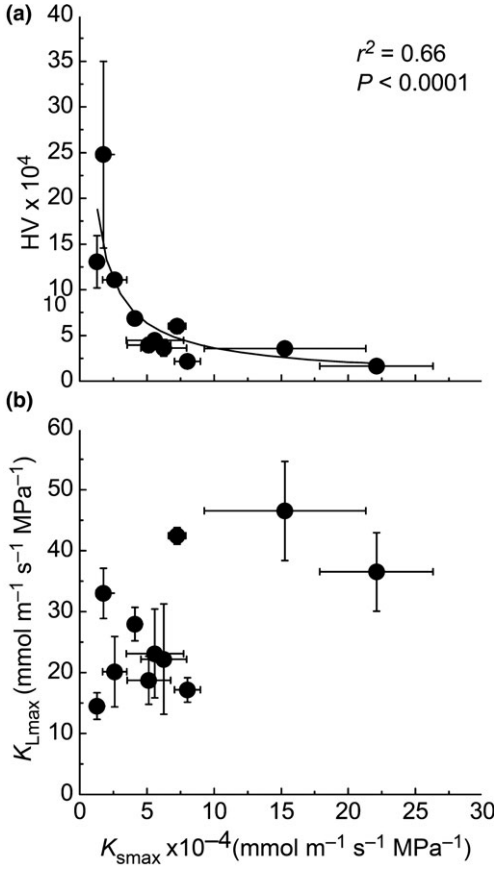

Fig. 3 Relationship between maximum sapwood-specific conductivity (K_{smax}) and Huber value (HV) (a), and K_{smax} and maximum leaf-specific conductivity (K_{Lmax}) (b). Each point is the mean from three individuals (n = 3) with error bar showing standard error.

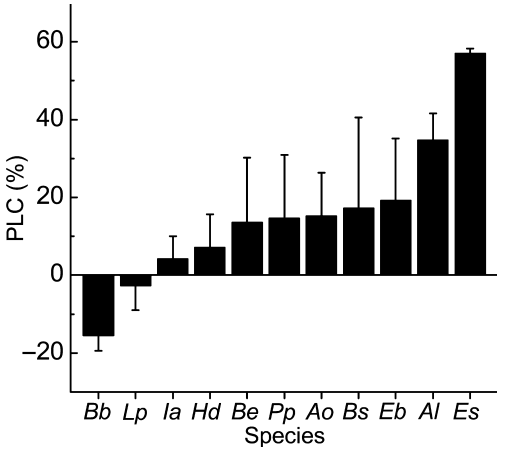

Fig. 4 Percentage loss of hydraulic conductivity (PLC) caused by freeze–thaw-induced embolism in stems of woody heath species. Bars show mean values from three individuals (n = 3) with error bar showing standard error. Abbreviations of the species' names are given in Table 1.

tively), although the linear regression explained less of the variation than the relationships between gas exchange parameters and K_{Lmax} (Fig. 6). Correlations were also found between A and D_h (r = 0.65, P = 0.03) and PLC (r = 0.73, P = 0.01) (Fig. 7).

Discussion

We observed coordination in a suite of traits governing resistance to freeze–thaw-induced embolism, hydraulic efficiency of the xylem and photosynthetic capacity of leaves in 11 heathland species. Across these species, significant positive relationships between leaf gas exchange (A and g_s) and K_L indicated that photosynthetic and hydraulic traits were highly interdependent. Vulnerability to freeze–thaw-induced embolism increased with K_s, a relationship driven by variations in xylem vessel characteristics; species more susceptible to freeze–thaw-induced embolism had wider and longer xylem vessels with lower vessel density per square millimetre. These results show that the tremendous variation in anatomy and physiology underlies a continuum of traits along which tolerance to freezing conditions is bal-

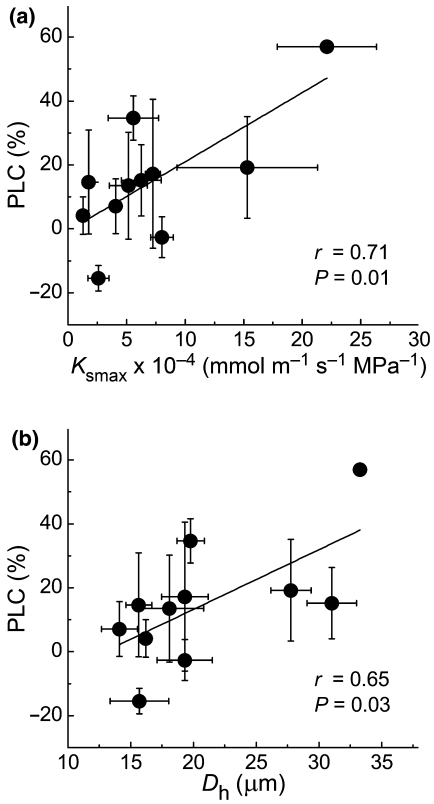

Fig. 5 Relationship between percentage loss of hydraulic conductivity (PLC) caused by freeze–thaw-induced embolism and maximum sapwood-specific hydraulic conductivity (K_{smax}) (a) and mean hydraulically weighted vessel diameter (D_h) (b). Each point is the mean from three individuals (n = 3) with error bar showing standard error.

anced by hydraulic efficiency and photosynthetic capacity, even during the winter. Notably, the heath vegetation at this high-elevation site maintained a significant degree of photosynthetic activity during a winter characterized by cool, above zero, daytime temperatures and high levels of hydration. Therefore, a significant potential for growth exists during the winter despite the regular imposition of freezing temperatures and the consequent possibility of freeze–thaw-induced cavitation.

Xylem anatomy, hydraulic efficiency and resistance to freeze–thaw-induced embolism

Xylem vessel diameter and length emerged as central to the coordination of traits linked to stress tolerance and productivity. In our dataset, there was a significant positive relationship between vessel diameter and maximum vessel length (Fig. 1). Although the full frequency distribution of vessel lengths was not measured, published distributions suggest that median and maximum vessel lengths tend to be well correlated (Zimmermann & Jeje, 1981; Sperry *et al.*, 2005). This xylem vessel allometry suggests that species with wider vessels should also have fewer vessel endings per unit length, and therefore the hydraulic resistance caused by intervessel pit crossings would be reduced as vessels become wider (Choat *et al.*, 2006). The number of vessels in cross-section per unit area decreased with increasing vessel diameter, a well-established trend following the geometric packing limit (Baas, 1986; McCulloh *et al.*, 2010; Zanne *et al.*, 2010). However, K_s increased with D_h and V_L despite lower vessel density, because of the exponential increase in conductivity with conduit diameter.

Wider conduit diameter was also associated with greater vulnerability to freeze–thaw-induced embolism, consistent with previous studies of both coniferous and angiosperm species (Sperry *et al.*, 1994; Davis *et al.*, 1999; Feild & Brodribb, 2001; Pittermann & Sperry, 2003; Cobb *et al.*, 2007; Stuart *et al.*, 2007). Here, we found a correlation within one community representing a continuum of freeze–thaw-induced PLC and vessel diameter, similar to that observed in Tasmanian heath species (Feild & Brodribb, 2001). Notably, none of the heath species in the present study exhibited the extreme vulnerability of ring porous species and vines in the Northern Hemisphere (Sperry *et al.*, 1994; Cobb *et al.*, 2007). Indeed, the heath species were relatively resistant to freeze–thaw-induced embolism, with the majority suffering PLCs of 20% or less in response to a −10°C freeze.

However, care must be taken when comparing results of different studies, given that the magnitude of tension and time of freezing can also be important factors in freeze–thaw-induced embolism (Davis *et al.*, 1999; Mayr *et al.*, 2007; Stuart *et al.*, 2007). For example, although, in our study, freeze–thaw-induced PLC values ranged from 20 to 60%, a previous study reported freeze–thaw-induced PLCs ranging from 40 to 80% for a range of angiosperm tree species with vessel diameters similar to those observed here (15–30 μm), including some congeners with our dataset, such as *Eucalyptus* and *Leptospermum* (Feild & Brodribb, 2001). However, in that study, branches were dehydrated to *c.* −0.5 MPa before the freeze–thaw treatment, whereas branches in the present study were frozen at the naturally occurring stem water potentials, which were high (i.e. mostly above −0.5 MPa) as a result of winter rainfall, and we saw no relationship between stem water potential before freezing and PLC. Thus, high water status may have contributed to the apparent high level of resistance to freeze–thaw-induced embolism in the heath species.

Coordination of stem hydraulic traits and leaf gas exchange

A strong positive relationship was observed between K_L and leaf gas exchange parameters (g_s and A) across the 11 species (Fig. 6). Such direct scaling between light-saturated photosynthetic rates and the maximum hydraulic conductivity of

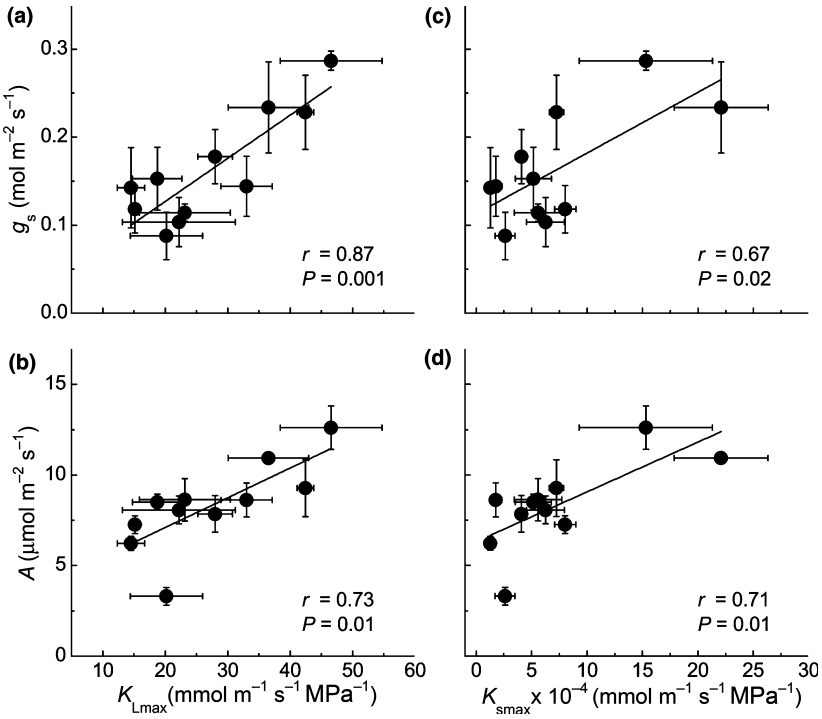

Fig. 6 Relationship between maximum leaf-specific hydraulic conductivity (K_{Lmax}) and stomatal conductance to water vapour (g_s) (a) and CO_2 assimilation rates (A) (c), and between maximum sapwood-specific conductivity (K_{smax}) and stomatal conductance to water vapour (g_s) (b) and CO_2 assimilation rates (A) (d), in 11 woody heath species. Each point is the mean from three individuals (n = 3) with error bar showing standard error.

stems (Santiago *et al.*, 2004; Lovelock *et al.*, 2006; Chen *et al.*, 2009) or leaves (Brodribb *et al.*, 2007) has been reported for a range of temperate and tropical species. We found that g_s and A were more closely related to K_L than K_s. Most previous studies have also found that gas exchange parameters are more closely related to K_L than to K_s, suggesting that the coordination of hydraulic supply and demand incorporates the allometry of the sapwood : leaf area ratio, rather than simply conforming to the hydraulic capacity of the stem xylem. In addition, HV decreased in a log-linear fashion with increasing K_s, indicating that a greater amount of leaf area was supported per cross-sectional area of stem as the efficiency of sapwood increased. Because changes in K_s are largely controlled by changes in vessel diameter and length, increasing vessel size was correlated with greater investment in leaf area for a given investment in sapwood tissue. This association is consistent with the idea that hydraulic traits related to whole-plant relative growth rates are part of a suite of coordinated traits, i.e. faster growing species have more allocation to leaf area relative to stem area for competitive light capture, as well as higher hydraulic and photosynthetic efficiency. Thus, the relationship between A and K_L is probably the result of a long-term coordination of hydraulic and photosynthetic traits, with far-reaching consequences for all aspects of plant morphology and function. The fact that the plants were in well-watered soil indicates that the correlation was not a result of differential stomatal closure across species to maintain hydraulic function. Rather, the relationship appears to reflect species optimizing maximum gas exchange relative to maximum hydraulic capacity, and this coordination is maintained when gas exchange and hydraulic conductance decline in the winter.

Conclusions

This study revealed strong integration between resistance to freezing stress and hydraulic and photosynthetic capacity across a functionally diverse range of overwintering broadleaf evergreens. Trade-offs were mediated by xylem anatomy, with narrow xylem vessel diameter correlated with resistance of stems to freeze–thaw-induced embolism, and higher rates of leaf gas exchange being related to greater hydraulic capacity (K_L and K_s), which was derived principally from wider xylem vessels. Trade-offs in hydraulic and photosynthetic capacity strongly imply that many of the shrub species would be limited in productivity by xylem traits that afford better resistance against freeze–thaw-induced embolism induced by episodic severe freezing events. By contrast, the taller stature *Eucalyptus* species exhibited higher photosynthetic rates that came at the expense of more significant losses of hydraulic capacity after freezing. Given the high water status of material examined in this study, the potential for more catastrophic loss of hydraulic capacity may accompany

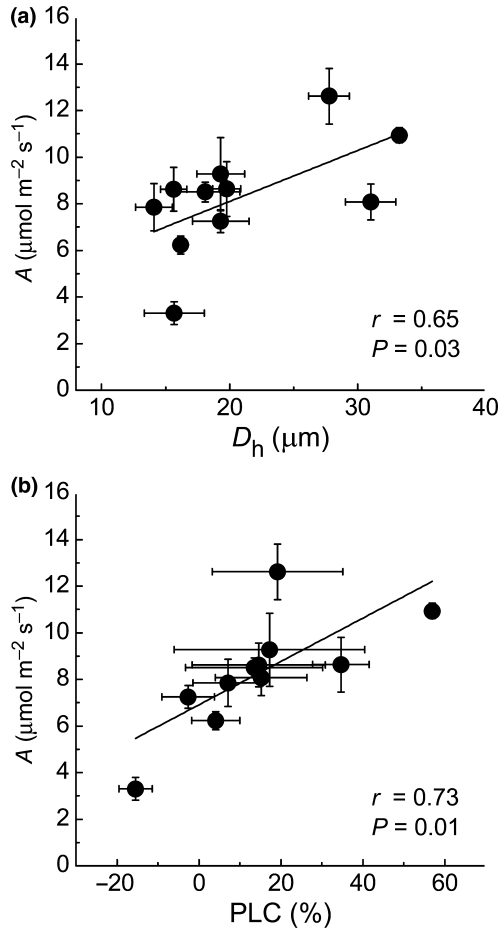

Fig. 7 Relationship between CO_2 assimilation rate (A) and hydraulically weighted vessel diameter (D_h) (a) and percentage loss of conductivity (PLC) caused by freeze–thaw-induced embolism (b) in 11 woody heath species. Each point is the mean from three individuals (n = 3) with error bar showing standard error.

unusually dry periods during the winter. This is of particular importance given predictions of greater variation in regional precipitation patterns.

Acknowledgements

This research was supported by Discovery Project Grant DP0881009 from the Australian Research Council to M.C.B. and L.S. We are grateful to Kanangra-Boyd National Park for permission to conduct the research.

References

Australian Bureau of Meteorology. 2011. [WWW document] URL http://www.bom.gov.au/climate/averages/tables/cw_063293.shtml [accessed 1 April 2011].

Baas P. 1986. Ecological patterns of xylem anatomy. In: Givnish TJ, ed. *On the economy of plant form and function*. Cambridge, UK: Cambridge University Press, 327–352.

Ball MC, Canny MJ, Huang CX, Egerton JJG, Wolfe J. 2006. Freeze/thaw-induced embolism depends on nadir temperature: the heterogeneous hydration hypothesis. *Plant, Cell & Environment* **29**: 729–745.

Ball MC, Egerton JJG, Leuning R, Cunningham RB, Dunne P. 1997. Microclimate above grass adversely affects spring growth of seedling snow gum (*Eucalyptus pauciflora*). *Plant, Cell & Environment* **20**: 155–166.

Blennow K, Lang ARG, Dunne P, Ball MC. 1998. Cold-induced photoinhibition and growth of seedling snow gum (*Eucalyptus pauciflora*) under differing temperature and radiation regimes in fragmented forests. *Plant, Cell & Environment* **21**: 407–416.

Brodribb TJ, Feild TS. 2000. Stem hydraulic supply is linked to leaf photosynthetic capacity: evidence from New Caledonian and Tasmanian rainforests. *Plant, Cell & Environment* **23**: 1381–1388.

Brodribb TJ, Feild TS, Jordan GJ. 2007. Leaf maximum photosynthetic rate and venation are linked by hydraulics[1[W][OA]]. *Plant Physiology* **144**: 1890–1898.

Brodribb TJ, Holbrook NM, Edwards EJ, Gutierrez MV. 2003. Relation between stomatal closure, leaf turgor and xylem vulnerability in eight tropical dry forest trees. *Plant, Cell & Environment* **26**: 443–450.

Castro-Diez P, Puyravaud JP, Cornelissen JHC, Villar-Salvador P. 1998. Stem anatomy and relative growth rate in seedlings of a wide range of woody plant species and types. *Oecologia* **116**: 57–66.

Cavender-Bares J, Holbrook NM. 2001. Hydraulic properties and freezing-induced cavitation in sympatric evergreen and deciduous oaks with contrasting habitats. *Plant, Cell & Environment* **24**: 1243–1256.

Chen JW, Zhang Q, Cao KF. 2009. Inter-species variation of photosynthetic and xylem hydraulic traits in the deciduous and evergreen Euphorbiaceae tree species from a seasonally tropical forest in south-western China. *Ecological Research* **24**: 65–73.

Choat B, Brodie TW, Cobb AR, Zwieniecki MA, Holbrook NM. 2006. Direct measurements of intervessel pit membrane hydraulic resistance in two angiosperm tree species. *American Journal of Botany* **93**: 993–1000.

Choat B, Cobb AR, Jansen S. 2008. Structure and function of bordered pits: new discoveries and impacts on whole-plant hydraulic function. *New Phytologist* **177**: 608–625.

Cobb AR, Choat B, Holbrook NM. 2007. Dynamics of freeze–thaw embolism in *Smilax rotundifolia* (Smilacaceae). *American Journal of Botany* **94**: 640–649.

Davis SD, Sperry JS, Hacke UG. 1999. The relationship between xylem conduit diameter and cavitation caused by freezing. *American Journal of Botany* **86**: 1367–1372.

Egerton JJG, Banks JCG, Gibson A, Cunningham RB, Ball MC. 2000. Facilitation of seedling establishment: reduction in irradiance enhances winter growth of *Eucalyptus pauciflora*. *Ecology* **81**: 1437–1449.

Feild TS, Brodribb T. 2001. Stem water transport and freeze–thaw xylem embolism in conifers and angiosperms in a Tasmanian treeline heath. *Oecologia* **127**: 314–320.

Franks PJ, Farquhar GD. 1999. A relationship between humidity response, growth form and photosynthetic operating point in C-3 plants. *Plant, Cell & Environment* **22**: 1337–1349.

Givnish TJ. 1986. *On the economy of plant form and function*. Cambridge, UK: Cambridge University Press.

Hacke UG, Sperry JS. 2001. Functional and ecological xylem anatomy. *Perspectives in Plant Ecology Evolution and Systematics* **4**: 97–115.

Hubbard RM, Ryan MG, Stiller V, Sperry JS. 2001. Stomatal conductance and photosynthesis vary linearly with plant hydraulic conductance in ponderosa pine. *Plant, Cell & Environment* **24**: 113–121.

Langan SJ, Ewers FW, Davis SD. 1997. Xylem dysfunction caused by water stress and freezing in two species of co-occurring chaparral shrubs. *Plant, Cell & Environment* **20**: 425–437.

Logullo MA, Salleo S. 1993. Different vulnerabilities of *Quercus ilex* L to freeze-induced and summer drought-induced xylem embolism – an ecological interpretation. *Plant, Cell & Environment* **16**: 511–519.

Lovelock CE, Ball MC, Choat B, Engelbrecht BMJ, Holbrook NM, Feller IC. 2006. Linking physiological processes with mangrove forest structure: phosphorus deficiency limits canopy development, hydraulic conductivity and photosynthetic carbon gain in dwarf *Rhizophora mangle*. *Plant, Cell & Environment* **29**: 793–802.

Mayr S, Cochard H, Ameglio T, Kikuta SB. 2007. Embolism formation during freezing in the wood of *Picea abies*. *Plant Physiology* **143**: 60–67.

McCulloh K, Sperry JS, Lachenbruch B, Meinzer FC, Reich PB, Voelker S. 2010. Moving water well: comparing hydraulic efficiency in twigs and trunks of coniferous, ring-porous, and diffuse-porous saplings from temperate and tropical forests. *New Phytologist* **186**: 439–450.

Meinzer FC, Goldstein G, Jackson P, Holbrook NM, Gutierrez MV, Cavelier J. 1995. Enivronmental and physiological regulation of transpiration in tropical forest gap species – the influence of boundary layer and hydraulic properties. *Oecologia* **101**: 514–522.

Miyazawa Y, Kikuzawa K. 2005. Winter photosynthesis by saplings of evergreen broad-leaved trees in a deciduous temperate forest. *New Phytologist* **165**: 857–866.

Mooney HA, Ehleringer JR 1997. Photosynthesis. In: Crawley MJ, ed. *Plant ecology*, 2nd edn. Cambridge, MA, USA: Blackwell Science, 1–27.

Pittermann J, Sperry J. 2003. Tracheid diameter is the key trait determining the extent of freezing-induced embolism in conifers. *Tree Physiology* **23**: 907–914.

Sack L, Holbrook NM. 2006. Leaf hydraulics. *Annual Review of Plant Biology* **57**: 361–381.

Sakai A, Larcher W. 1987. *Frost survival of plants: responses and adaptation to freezing stress*. New York, USA: Springer-Verlag.

Santiago LS, Goldstein G, Meinzer FC, Fisher JB, Machado K, Woodruff D, Jones T. 2004. Leaf photosynthetic traits scale with hydraulic conductivity and wood density in Panamanian forest canopy trees. *Oecologia* **140**: 543–550.

Sperry JS, Hacke UG, Wheeler JK. 2005. Comparative analysis of end wall resistivity in xylem conduits. *Plant, Cell & Environment* **28**: 456–465.

Sperry JS, Nichols KL, Sullivan JEM, Eastlack SE. 1994. Xylem embolism in ring-porous, diffuse-porous, and coniferous trees of northern Utah and interior Alaska. *Ecology* **75**: 1736–1752.

Sperry JS, Sullivan JEM. 1992. Xylem embolism in response to freeze–thaw cycles and water stress in ring-porous, diffuse-porous, and conifer species. *Plant Physiology* **100**: 605–613.

Stuart SA, Choat B, Martin KC, Holbrook NM, Ball MC. 2007. The role of freezing in setting the latitudinal limits of mangrove forests. *New Phytologist* **173**: 576–583.

Tyree MT, Zimmermann MH. 2002. *Xylem structure and the ascent of sap*. New York, USA: Springer-Verlag.

Wang J, Ives NE, Lechowicz MJ. 1992. The relation of foliar phenology to xylem embolism in trees. *Functional Ecology* **6**: 469–475.

Xin Z, Browse J. 2000. Cold comfort farm: the acclimation of plants to freezing temperatures. *Plant, Cell & Environment* **23**: 893–902.

Zanne AE, Westoby M, Falster DS, Ackerly DD, Loarie SR, Arnold SEJ, Coomes DA. 2010. Angiosperm wood structure: global patterns in vessel anatomy and their relation to wood density and potential conductivity. *American Journal of Botany* **97**: 207–215.

Zhang JL, Cao KF. 2009. Stem hydraulics mediates leaf water status, carbon gain, nutrient use efficiencies and plant growth rates across dipterocarp species. *Functional Ecology* **23**: 658–667.

Zimmermann MH, Jeje AA. 1981. Vessel-length distribution in stems of some American woody-plants. *Canadian Journal of Botany-Revue Canadienne de Botanique* **59**: 1882–1892.